ELSEVIER

Studies on the aggregation-induced emission of silole film and crystal by time-resolved fluorescence technique

Yan Ren [a,c], Yongqiang Dong [b], Jacky W.Y. Lam [b],
Ben Zhong Tang [b], Kam Sing Wong [a,*]

[a] Departments of Physics, The Hong Kong University of Science and Technology, Clear Water Bay, Kowloon, Hong Kong, SAR PR China
[b] Departments of Chemistry, The Hong Kong University of Science and Technology, Clear Water Bay, Kowloon, Hong Kong, PR China
[c] State Key Laboratory of Crystal Materials, Shandong University, Jinan, 250100, PR China

Abstract

In this Letter, the photoluminescence of 1,1,2,3,4,5-hexaphenylsilole (HPS) and poly{1,1-[(1,2,3,4,5-pentaphenylsiloly)oxy]-1-phenyl-1-undecyne} (PS9PA) was studied in detail by time-resolved fluorescence technique to investigate possible mechanisms of their unique aggregation-induced emissions. Enhanced emissions and long lifetimes of HPS and PS9PA films were detected in PMMA matrix compared to those of their solutions. Furthermore, strong fluorescence with nanosecond lifetimes was also obtained in the single crystal of HPS. These results show that intramolecular vibrational and torsional motions can act as efficient nonradiative pathways for the excited states to decay in the solutions and that suppression of these motions by restricting intramolecular vibrations in the solid state leads to enhanced fluorescence.

1. Introduction

Recently, siloles have been found to exhibit unusual aggregation-induced emission (AIE) properties [1]. They are weakly luminescent or practically nonluminescent in solutions, but become highly emissive in their aggregates. The fluorescence quantum yields of siloles in aggregates rise by a few hundred times, compared to those in solutions. Organic luminophores with AIE properties are promising materials for electroluminescence (EL) applications because in the EL devices, the luminescent materials are used in a form of thin film and scientists have tried hard to mitigate the problem of light emission quenching by aggregates in these devices [2]. It is therefore understandable why the AIE in siloles attracted immediate attention when it had been

report [3]. Another advantage of using silole for EL application is that it possesses very high electron mobility. Although extensive research has been carried out, very few organic materials have been found to show high electron mobility. In fact, high external quantum efficiency up to 8% was demonstrated in organic light emitting diode using silole as the emissive and electron transport layer [4–6]. Some other compounds have been subsequently reported to exhibit AIE properties [7–9]. The unusual photoluminescence (PL) properties also arouse researchers' interests in their physical origins. But, as yet, there are still no common opinions about the exact mechanism of the AIE [7–11]. For the AIE of siloles, the suggested mechanism is based on a restricted intramolecular motion model. It proposes that the nonradiative channel via the vibrational/torsional energy relaxation processes is blocked in the aggregate state and that this blockage enhances the radiative recombination of the excited state [6,11–13].

* Corresponding author. Fax: +852 2358 1652.
E-mail address: phkswong@ust.hk (K.S. Wong).

In this Letter, we try to further investigate the possible mechanism of AIE. The samples of HPS and PS9PA in two aggregate states, i.e., thin film and single crystal, have been prepared in order to examine the real role of the restriction of intramolecular motions in the AIE of the siloles. Time-resolved fluorescence technique was used to elucidate the mechanism of luminescence by comprehensive and quantitative understanding of the recombination dynamics and deactivation processes of molecular excited states. The new experimental results obtained from the time-resolved fluorescence behaviors of the silole film and single crystal provide further direct evidences for the restricted intermolecular motion model.

2. Experimental

The molecular structures of HPS and PS9PA are given in Fig. 1. Benzene solutions of HPS and PS9PA were prepared for absorption and PL measurements. The film samples for PL measurements were prepared by spin coating chloroform solutions of HPS/PMMA and PS9PA/PMMA (1:1) on clean glass substrates. After the solvent was evaporated, films of good quality were obtained. The single crystal of HPS was obtained by solution grown technique from the chloroform solution of HPS/PMMA (1:1).

The UV absorption spectra were measured on a Shimadzu UV-2401 spectrophotometer. A quartz cell of 1 cm thickness was used in the solution measurement. The absorption spectra of the solutions are shown in Fig. 1. The absorption peak of HPS is located at ∼367 nm, while that of PS9PA is red-shifted by ∼9 nm. The absorption spectra of the films of HPS and PSPA are essentially the same as those of their solutions.
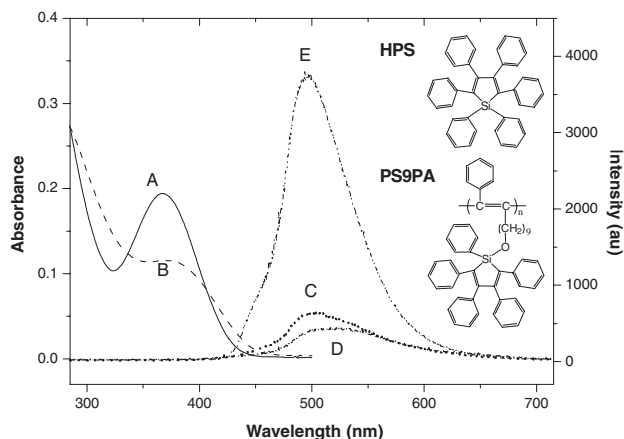

Fig. 1. UV absorption spectra of benzene solutions (22 μM) of HPS (A) and PS9PA (B) and PL spectra of benzene solutions (2 wt%) of HPS (C) and PS9PA (D) and single crystal of HPS (E).

Laser pulses of 267 nm were used as the excitation light source for the PL measurements. This was produced by the frequency summation of 800 nm with its 400 nm frequency-doubling from a Ti:sapphire regenerative amplifier (200 fs pulse width and 1 kHz repetition rate). For time-resolved fluorescence measurements, the fluorescence signals were collimated and focused onto the entrance slit of a monochrometer with the output plane connected to a synchroscan streak camera (Hamamatsu C4334, 25 ps system resolution). The fluorescence spectra of the silole samples were measured on a fiber spectrometer (Ocean Optics Inc.) to record the time-integrated PL spectra before each run of lifetime measurement. The laser pulse energy used for excitation was ∼0.5 μJ or lower. As shown in Fig. 1, the PL spectra of the HPS and PS9PA solutions are peaked at 498 and 517 nm, respectively. On the other hand, the emission peaks of HPS and PS9PA films were slightly blue-shifted and narrower compared with their respective solution. The time-resolved PL signals were therefore analyzed at these peak positions.

3. Results and discussion

The time-resolved fluorescence spectra of the benzene solutions and thin films of HPS and PS9PA are shown in Fig. 2. The dotted lines are the experimental data and the solid lines are the fitting curves based on exponential functions. From Fig. 2, one can see that the fluorescence of the benzene solution of HPS decays very fast compared to that of its film. The lifetime data is shown in Table 1. The HPS solution fluorescence shows single exponential decay with emission lifetime as short as ∼60 ps, which is close to the limit of the resolution of the streak camera system (∼25 ps). This result is consistent with the time-correlated photon counting measurement by Lee et al. [14] where the fluorescence decay of HPS in pure solvent is barely resolved by 150 ps instrument response function.

For the HPS film, the following double-exponential function

$$y = A_1 e^{-t/\tau_1} + A_2 e^{-t/\tau_2}$$

can simulate its decay behavior better than does the single-exponential one. This reveals that the excited states of HPS molecules in the film decay through two pathways. The values of A_1 and A_2 in the above function represent the fractions of molecules decaying in the two pathways. As shown in Table 1, 37% of HPS molecules in film decay through the fast pathway, whose lifetime are 120 ps. However, there are 63% of molecules decay through the slow pathway, whose lifetime is 1.46 ns, which is more than 20-fold longer than that of HPS in
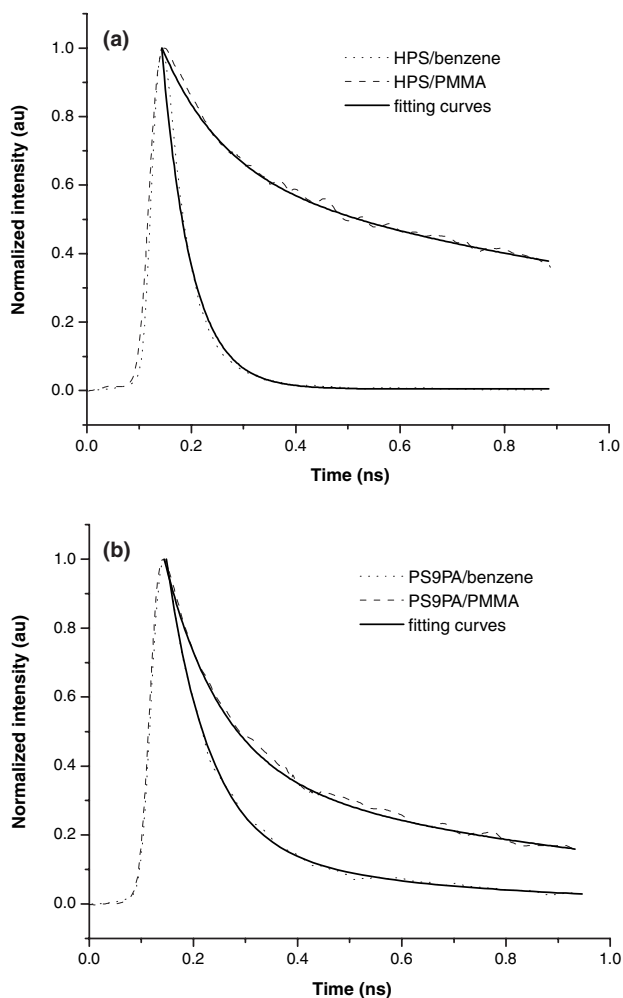
Fig. 2. Time-resolved fluorescence spectra of (a) 2 wt% HPS/benzene solution (dotted line) and 1:1 HPS/PMMA film (dashed line) and (b) 2 wt% PS9PA/benzene solution (dotted line) and 1:1 PS9PA/PMMA film (dashed line). The solid lines are the fitting curves based on single- (for HPS solution) and double-exponential functions.

Table 1
PL lifetimes of the benzene solutions (2 wt%) of HPS and PS9PA (2 wt%), the thin films of HPS and PS9PA blended with PMMA (in 1:1 ratio), and the single crystal of HPS

	HPS			PS9PA		
	A_1/A_2	τ_1 (ns)	τ_2 (ns)	A_1/A_2	τ_1 (ns)	τ_2 (ns)
Solution	1/0	0.06		0.82/0.18	0.08	0.43
Film	0.37/0.63	0.12	1.46	0.61/0.39	0.11	0.87
Crystal	0.44/0.56	1.22	5.20			

solution (60 ps). The slow pathway becomes the main relaxation channel in the light-emitting process of the HPS film. By contrast, the relaxation of the excited states of HPS in solution is solely through the fast deactivation process. Similar features can be seen in the time-decay behaviors of PS9PA. The PS9PA film also exhibits longer lifetime in comparison to the solution sample. However, different from HPS, both the fast

and slow deactivations participate in the relaxation process of PS9PA in solution. We consider that the difference between HPS and PS9PA mainly originate from the difference in their molecular structures. For PS9PA, the silole group is attached to the polyacetylene backbone as a pendant and therefore there is an issue of speed of the excited state energy transfer from the backbone to the pendant. Furthermore, the polymer may coil around even in solution, which will affect the intramolecular motion of the silole group. In addition, it is known that the viscosity of the solvent strongly influences the PL yield and emission lifetime of silole [12,15] and the change in the viscosity of 2 wt% polymer solution is another possible reason that influences the recombination dynamics. But one can see that in Table 1, majority of excited states of PS9PA in solution still decays through the fast pathway, with a PL lifetime of only ~80 ps. Therefore, it is the fast decay that dominates the deactivation of excited states of PS9PA in solution, which is as same as that of HPS.

How to understand the difference of the time-decay behaviors of siloles in between solution and film? It is known that the PL lifetime τ is related to radiative (τ_r) and nonradiative (τ_{nr}) lifetimes by the expression $1/\tau = 1/\tau_r + 1/\tau_{nr}$, in which τ_r is the intrinsic property of the molecule and is a constant. The short lifetime and low PL yield of siloles in solution hints that there is a strong nonradiative recombination process in the relaxation of their excited states. Vibrational and torsional energy relaxations are known to nonradiatively deactivate the excited species [16–20]. In solution, the motions of molecules are easy. Little restrictions are imposed on the molecular vibrational/torsional movements. Consequently, the excited states of molecules are easily annihilated through this nonradiative deactivation process. On the other hand, the probability of molecular vibration/torsional motion is low in film. As a result, the relaxation of the excited states through the radiationless channel is well blocked. The radiative recombination becomes the dominant decay channel of the excited states, which enhances the emission efficiency and increases the PL lifetime of the silole film or aggregate.

It is well known that the radiative lifetime τ_r of molecules can be calculated from the absorption and emission spectra using Strickler–Berg formula [21] given by

$$\frac{1}{\tau_r} = \frac{9.61 \times 10^{-20} n^2}{c^2} \langle v^{-3} \rangle^{-1} \int \varepsilon \, d \ln v$$

and

$$\langle v^{-3} \rangle^{-1} = \frac{\int I(v) \, dv}{\int v^{-3} I(v) \, dv},$$

where the multiplicities of the lower (ground) and upper (emitting) states are ignored. In the above equa-

tions, ε is the molar extinction coefficient, c is the speed of light in vacuum (in unit of cm/s), n is the refractive index of the medium, v is the frequency and I is the intensity of the fluorescence spectrum. Using the Strickler–Berg formula, the τ_r is calculated to be 13 ns for HPS in benzene solution. The PL lifetime τ is given by $\tau = \phi\tau_r$, where ϕ is the quantum efficiency ($\phi \approx 0.001$ for HPS in benzene and other pure solvents [11]), thus the calculated τ is 13 ps. Consider that we have ignored the multiplicities term and the approximations made in this model, as well as the relatively large Stokes shift of the PL from the absorption peak; the calculated lifetime $\tau = 13$ ps is in reasonable agreement with the measured lifetime of 60 ps. This result again confirmed that the ultrafast excited state lifetime of HPS in solvent is due to some very efficient nonradiative process, and in this case it is the result of nonradiative excited state relaxation mediated by intramolecular vibrational/torsional motions. Comparing the measured and calculated PL lifetime of PS9PA is more difficult because of the multi-component PL decay. However, Strickler–Berg calculation results in $\tau_r = 15$ ns for PS9PA and with quantum yield of 0.0069 so that the calculated τ is 103 ps, which is in very good agreement with the fast decay component of measured PL lifetime.

If the above analysis is right, a strong fluorescence should be obtained from the crystal of siloles due to its high chromophore density and because the crystalline packing severely restricts the vibrational/torsional motion of the phenyl rings. The experiment on the PL properties of HPS single crystal was thus performed. As expected, strong fluorescence was emitted from the crystal after it was excited by a laser beam. The photographs taken during the experiment are shown in Fig. 3. One can see the very bright blue-green light emission from the HPS crystal. The fluorescence spectrum is shown in Fig. 1. The PL peak is located at ~497 nm, which is essentially the same as that of the HPS solution. Fig. 4 shows the time-resolved fluorescence spectra of the single crystal. The PL lifetime is very long and it also decays through two pathways as shown by the double-exponential decay fitting. Table 1 gives the lifetime constants of the two decay components. Although there is 44% of molecules decay through the 'fast' pathway, this 'fast' PL lifetime is as long as 1.22 ns, which is comparable to the slow decay component in the HPS film (1.46 ns). The other 56% of the excited molecules decay through the slow pathway with a time constant of 5.20 ns, which is almost 90 times longer than that of HPS in solution.

It was suggested that planarization of a silole molecule upon formation of aggregate [10] might have caused this enhanced emission [1]. However, ground state silole is actually nonplanar as indicated by the crystal structure determined by X-ray diffraction (Fig. 5) [11], thus
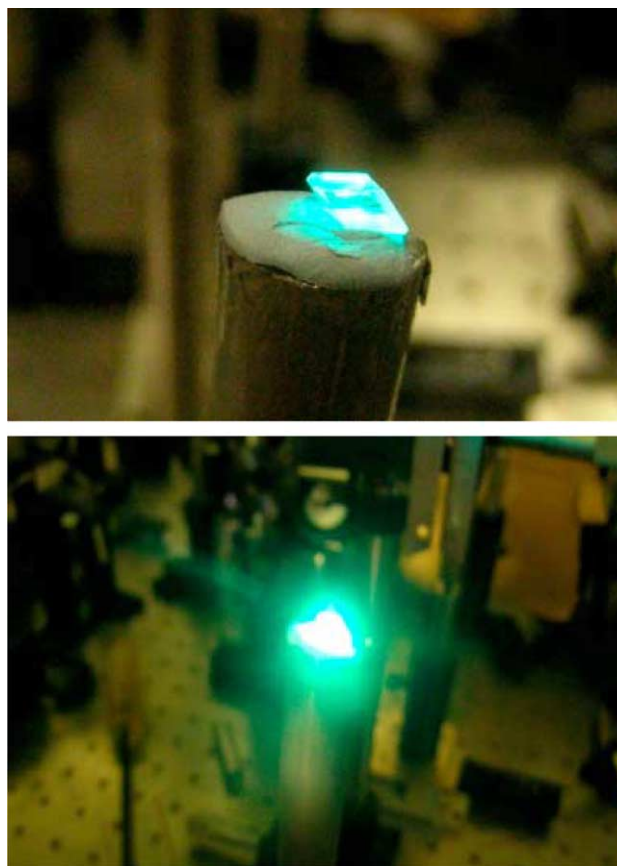

Fig. 3. Upper panel: single crystal of HPS measured 4 mm × 3 mm × 2 mm by size. Lower panel: strong fluorescence emitted from the single crystal when it is excited by a 400-nm, 1-KHz, and 200-fs Ti:sapphire regenerative laser beam.
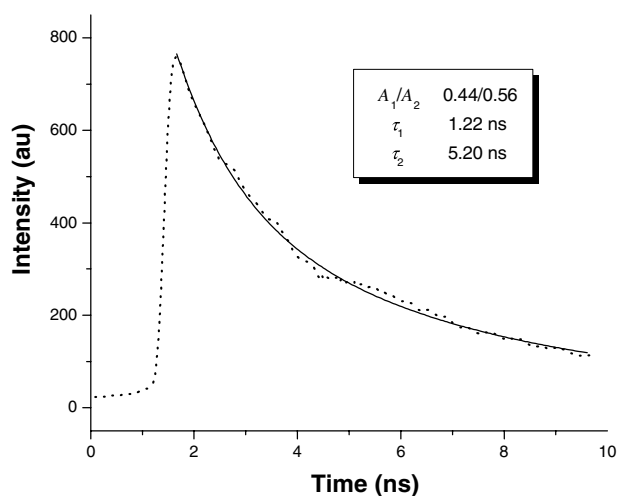

Fig. 4. Time-resolved fluorescence of the single crystal of HPS (dotted line). The solid line is the fitting curve based on the double-exponential function.

this enhanced emission due to planarization in aggregate state can be ruled out. Fig. 5 shows that the silole crystal has two molecules in one unit cell, in which the adjacent
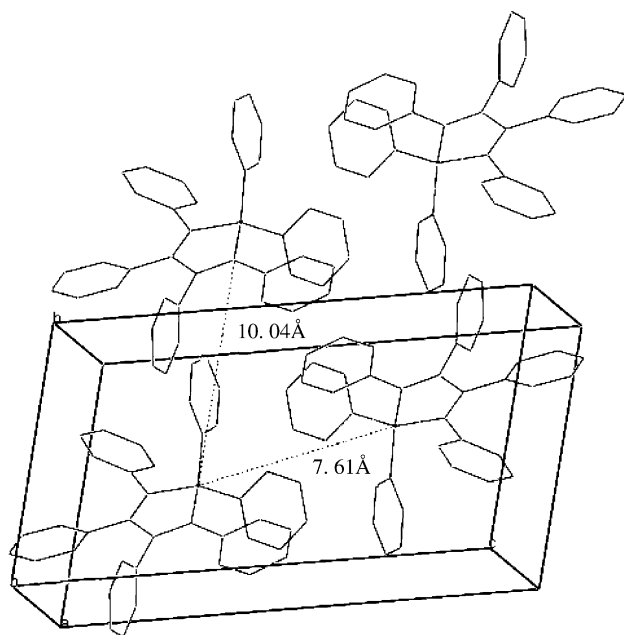
Fig. 5. Packing diagram of HPS single crystal, where the interplane distance is 10.04 Å and the intermolecular distance within the unit cell is 7.61 Å.

phenyl rings as well as the phenyl and silole rings are nonplanar due to steric hindrance. In addition, it is well know that well packed aggregates of polar molecules with strong π–π stacking tends to prevent radiative recombination. However, the distinct nonplanar structure of the silole molecule in solid state formed with an interplane molecular distance of ~ 10 Å prevents effective π–π stacking as shown in Fig. 5. This suppresses the intermolecular interaction that tends to induce nonradiative recombination as seen in the 'normal' aggregates with strong π–π stacking interactions.

Radiationless transition of the exciton of a molecule can be via internal conversion from singlet excited state to singlet ground state (S_1–S_0) or intersystem crossing from singlet excited state to triplet excited state (S_1–T_1). The S_1–S_0 and S_1–T_1 nonradiative relaxations are often mediated by vibrational, rotational and torsional motions of the molecule. Restriction of these motions will affect the excited state nonradiative recombination rate and enhance the emission efficiency. For S_1–T_1 intersystem crossing, the energy transfer process is very sensitive to the energy level of the triplet state relative to the singlet state. The different degrees of twisting of the phenyl rings of the silole from planar structure in solution and solid states may also affect the triplet state level and consequently the rate of S_1–T_1 nonradiative relaxation. Experiments are currently underway to determine the triplet state levels of the silole solutions and films. Nevertheless, our results clearly indicate that the restricted motion of the phenyl rings of the siloles in the film and crystal enhances the radiative recombination.

4. Conclusions

The time-resolved fluorescence reveals that the nonradiative deactivation channel dominates the excited state relaxation process of the siloles in solution, which is effectively blocked in aggregates due to the restrictions of molecular vibrational and torsional motions. The fluorescence of the siloles is greatly enhanced in crystal as well as in film. The experimental results from the time-resolved fluorescence measurement provide further direct evidences for the restricted intramolecular motion model for the explanation of the novel AIE phenomena of siloles.

References

[1] J.D. Luo, Z.L. Xie, J.W.Y. Lam, L. Cheng, H.Y. Chen, C.F. Qiu, H.S. Kwok, X.W. Zhan, Y.Q. Liu, D.B. Zhu, B.Z. Tang, Chem. Commun. (2001) 1740.
[2] R.H. Friend, R.W. Gymer, A.B. Holmes, J.H. Burroughes, R.N. Marks, C. Taliani, D.D.C. Bradley, D.A. dos Santos, J.L. Brédas, M. Lögdlund, W.R. Salaneck, Nature 397 (1999) 121.
[3] M. Freemantle, Chem. Eng. News 79 (41) (2001) 29.
[4] L.C. Palilis, A.J. Mäkinen, M. Uchida, Z.H. Kafafi, Appl. Phys. Lett. 82 (2003) 2209.
[5] H. Murata, G.G. Malliaras, M. Uchida, Z.H. Kafafi, in: G.E. Jabbour, N.S. Sariciftci (Eds.) MRS Symposium Proceeding 'Electronic, Optical and Optoelectronic Polymers and Oligomers', vol. 665, Material Research Society 2001, p. 227.
[6] H.Y. Chen, J.W.Y. Lam, J.D. Luo, Y.L. Ho, B.Z. Tang, D. Zhu, M. Wong, H.S. Kwok, Appl. Phys. Lett. 81 (2002) 574.
[7] B. Manimaran, P. Thanasekaran, T. Rajendran, R.J. Lin, I.J. Chang, G.H. Lee, S.M. Peng, S. Rajagopal, K.L. Lu, Inorg. Chem. 41 (2002) 5323.
[8] B.K. An, S.K. Kwon, S.D. Jung, S.Y. Park, J. Am. Chem. Soc. 124 (2002) 14410.
[9] S. Jayanty, T.P. Radhakrishnan, Chem. Eur. J. 10 (2004) 791.
[10] M. Levitus, K. Schmieder, H. Ricks, K.D. Shimizu, U.H.F. Bunz, M.A. Garcia-Garibay, J. Am. Chem. Soc. 123 (2001) 4259.
[11] J. Chen, C.C.W. Law, J.W.Y. Lam, Y. Dong, S.M.F. Lo, I.D. Williams, D. Zhu, B.Z. Tang, Chem. Mater. 15 (2003) 1535.
[12] J. Chen, Z. Xie, J.W.Y. Lam, C.C.W. Law, B.Z. Tang, Macromolecules 36 (2003) 1108.
[13] J. Chen, H. Peng, C.C.W. Law, Y. Dong, J.W.Y. Lam, I.D. Williams, B.Z. Tang, Macromolecules 36 (2003) 4319.
[14] M.H. Lee, D. Kim, Y. Dong, B.Z. Tang, J. Korea, Phys. Soc. 45 (2004) 329.
[15] Y. Ren, Jacky W.Y. Lam, Y.Q. Dong, B.Z. Tang, K.S. Wong, J. Phys. Chem. B (in press).

[16] J. Malkin, Photophysical and Photochemical Properties of Aromatic Compounds, CRC Press, Boca Raton, FL, 1992.

[17] D.L. Wise, G.E. Wnek, D.J. Trantolo, T.M. Cooper, J.D. Gresser, Photonic Polymer Systems, New York, 1998.

[18] K.S. Wong, H. Wang, G. Lanzani, Chem. Phys. Lett. 288 (1998) 59.

[19] Y. Li, G. Vamvounis, S. Holdcroft, Macromolecules 35 (2002) 6900.

[20] Y. Kanemitsu, K. Suzuki, Y. Masumoto, Phys. Rev. B 50 (1994) 2301.

[21] S.J. Strickler, R.A. Berg, J. Chem. Phys. 37 (1962) 814.